Smart Foam Cement Quality Control and Behavior Characterized Using Artificial Neural Network and Vipulanandan Models

Professor C. Vipulanandan Ph.D., P.E.
"**Smart Cement**" Inventor and Text Book
"**Vipulanandan Rheological Model**"
"**Vipulanandan Failure Model**"
Chief Editor – Advances in Civil Engineering
Director, Center for Innovative Grouting Material and Technology (CIGMAT)
Director, Texas Hurricane Center for Innovative Technology (THC-IT)
Professor of Civil and Environmental Engineering
University of Houston, Houston, Texas 77204-4003

Abstract

There is increasing interest in using light weight cement slurries with foam additions for multiple applications including onshore and offshore deep wells installed in varying and challenging geological formations with low strength rocks. Recently highly sensing smart foam cement has been developed to real-time monitor the changes in the material. Also, the foam cement has reduced thermal conductivity making it a better insulator. It is also important to model the behavior of the smart foam cement for real time monitoring with the artificial neural network (ANN) models for adaptation in machine learning for various applications. The investigation was on the performance of highly sensing foam added smart cement and verified with various behavior models. Highly sensing smart oil well cement with water to cement (w/c) ratio of 0.38 was modified by adding 5% and 20 % foam by weight and was first characterized using the impedance–frequency response to identify the critical electrical property for monitoring. Based on the Vipulanandan Impedance Model, electrical resistivity was the monitoring property. For quality control of the mixing in the field the electrical resistivity can be used and with 5% and 20 % foam addition electrical resistivity increased by 14% and 94% and Vipulanandan correlation model was used to relate the density to the resistivity. Also rheological properties and piezoresistivity (slurry) were investigated. With the addition of 20% foam the smart foam cement density reduced by 45% and the thermal conductivity reduced by 65%.With the addition of 20% foam the initial resistivity increased by 94% indicating a potential quality control parameter for monitoring in the field. The thermal conductivity and the initial resistivity were related to the density using the Vipulanandan Correlation Model. The slurries investigated were piezoresistive, when pressure was applied the electrical resistivity changed. The rheological behavior of the smart foam cement slurries have been quantified using the new Vipulanandan rheological model and compared with Artificial Neural Network (ANN) Model. The slurry piezoresistivity model was used to predict the piezoresistive behavior and compared it to an ANN model. The accuracy of the all the

model predictions were compared using the statistical parameters such as the root mean square error (RMSE) and the coefficient of determination.

Introduction

The oil and gas wells are going deeper and deeper to be more productive but are going into highly varying geological formations creating challenges in onshore and offshore well construction beginning at the ground level and seafloor respectively. Also the cement systems used in these well constructions must be lighter density with good fluid loss characteristics to be circulated in place during construction (Bour et al. 2000). Minimizing the fluids loss has become a critical issue to make sure the wellbore integrity because of the varying geological and environmental conditions in the ground [Labibzadeh et al. 2010, Ravi et al. 2007, Fuller et al. 2002). Also the cement to be environmental friendly is important (Thaemlitz et al. 1990). In 2010 there was a major oil well failure in the Gulf of Mexico and one of the main contributing factors that caused this event was the light weight cement, which did not set properly in the deep well (Carter et al. 2014). Many of the oil well failures both onshore and offshore are caused by cement failures (Izon et al. 2007). There is a need for real-time monitoring not only the cementing operations and but also the performance during the entire service life (Vipulanandan et al. 2015-2020).

In order to monitor and characterize the condition of cementitious materials several nondestructive methods (impact-echo, pulse-echo, ultrasonic pulse velocity wave reflection, resonant frequency, acoustic emission and microwave adsorption) have been used (Zhang et al. 2009, Vipulanandan et al. 2018b, Ichim et al. 2019). Use of these methods have two major drawbacks. Firstly, these methods only give snap shot of the data and do not provide any kind of continuous real time monitoring. Secondly, implementation of all these techniques in the field require temporary stopping of the well operations. Recently, nondestructive real time monitoring system with monitoring the cement sheath from outside the casing using instrumentation was developed by using electrical resistivity measurements (Vipulanandan et al. 2018a, Vipulanandan 2021). Vipulanandan has developed the highly sensing smart cement with real time monitoring ability using electrical resistivity as the sensing property to quantify changes in the cement due to pressures, temperatures, contaminations, corrosion and cracking (U.S. Patent 2019). Increasing depth of the oil wells is leading designing of cement mixtures with different formulations. Due to the presence of weak formations and lost circulation zones, cementing these formations with regular heavy slurries pose many challenges.

Lightweight Slurries

As fragile formations cannot withstand hydrostatic pressure caused by the regular heavy cement slurries, use of light weight slurries are becoming popular (Ahmadi et al. 2013, Glosser et al. 2016). Ultra-light weight cements have been used in areas of weak formations (Harness 1992). Past studies as have shown that the use of Class G and Class H Oil well cements for preparation of light weight slurries is popular [Smith et al. 1984, Loeffler et al. 1984, Rickard 1985, Harms et al. 1985, Dusterhoft 2003, Sugama et al. 2005, Marriot 2005). Also, light weight cements were prepared to reach a target density of about 0.7 to 1.2g/cc. This range of densities was produced by foaming the light weight cements.

The various types of light weight additives such as silica flour, bentonite, microspheres and nitrogen foam have been used (Rickard 1985, Harms et al. 1985).

Of all the studies, there were very few details on the electrical characterization of light weight cement slurries. Also, foamed cement has the advantage of being squeezed into high permeability zones where lost circulation is common. Foamed cement slurries have been accepted all around the world and were monitored using cement bond logs and ultrasonic cement evaluation (Hill 1990, McCarter et al. 2000). The smart foamed cement can be used for real-time monitoring while it sustains its structural properties. Electrical resistivity has been considered as a monitoring parameter since it is a material property, which is sensitive to the changes inside the material, during setting and hardening (McCarter et al. 2000).

There is emerging interest in developing and characterizing the performance properties of smart foamed cements. Preparation of smart foamed cement material sensitive to stresses, temperatures, cracks, contaminations enables us to monitor the changes in the material with high accuracy. Hence, it is important to experimentally evaluate the performance of these materials.

Artificial Neural Networking (ANN)

ANN is a computational model that is more like of human brain ~~like~~ learning system, also referred as Artificial Intelligent (AI). Essentially ANN is more of educated and adaptive system that trains itself to predict solutions (Dahnoune et al. 2015, Hammoudi et al 2019). The ANN studies were first started in 1943 followed by further development by Rosenblatt in 1958. Rosenblatt developed machine named the "perceptron" which consisted of sensory units connected to single layer of neurons. The learning algorithm for the perceptron network was call back propagation with hidden units. As a result of developments in computer technology and recent advancements, ANN has become an efficient and powerful tool. (Topcu 2008). Other application sectors include airline security, industrial process control, stock exchange, data validation and others (Demircan et al. 2011, Mishra et al. 2014).

The approach is based on back propagation weight update rule. Generally, an input layer is propagated through the network which has set of weights to predict the output. The objective of the training or learning is to adjust the weights so that the difference between expected output and predicted output is minimal. This basically involves reduction of the absolute error. Back propagation is such an algorithm that performs a gradient descent minimization of squared error (Arnavat et al. 2015).

Material Characterization

It is important to identify the critical material properties that can be easily monitored in the field. Compared to the physical and chemical properties of the material the electrical properties can be easily monitored in the field.

Vipulanandan Impedance Model

It is important to identify the most appropriate equivalent circuit to represent the electrical properties of a material to characterize its performace with time [Vipulanandan et al. 2013, Vipulanandan 2021). In this study, different possible equivalent circuits were

analyzed to find an appropriate equivalent circuit to represent smart cement with and without foam.

analyzed to find an appropriate equivalent circuit to represent smart cement with and without foam.

CASE 1: General Material – (Resistance and Capacitance)

In CASE-1, both the contacts and the bulk material are represented using a resistor and capacitor connected in parallel (Figure 1).In the equivalent circuit for CASE 1, bulk material resistance (R_b) and capacitance (C_b) and R_c and C_c are resistance and capacitance of the contacts, respectively. The impedance for CASE 1 (Z_1) is represented as follows :

$$Z_1(\sigma) = \frac{R_b(\sigma)}{1+\omega^2 R_b^2 C_b^2} + \frac{2R_c(\sigma)}{1+\omega^2 R_c^2 C_c^2} - j\left\{\frac{2\omega R_c^2 C_c(\sigma)}{1+\omega^2 R_c^2 C_c^2} + \frac{\omega R_b^2 C_b(\sigma)}{1+\omega^2 R_b^2 C_b^2}\right\}, \quad (1)$$

where ω is the angular frequency of the applied signal. When the frequency is very low, $\omega \rightarrow 0$, $Z_1 = R_b + 2R_c$, and when it is very high, $\omega \rightarrow \infty$, $Z_1 = 0$.

CASE 2: Resistance Material

This will be a special case of CASE-1 in which the capacitance of the bulk material (C_b) is zero (Figure 2). The impedance for CASE-2 (Z_2) is as follows:

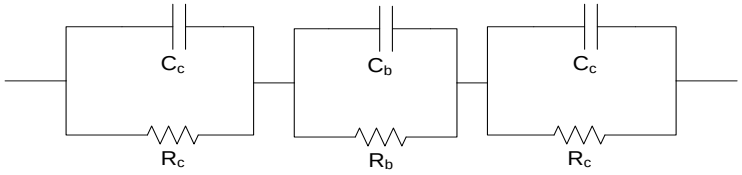

Figure 1 Representative Electrical Circuit for CASE-1

$$Z_2(\sigma) = R_b(\sigma) + \frac{2R_c(\sigma)}{1+\omega^2 R_c^2 C_c^2} - j\frac{2\omega R_c^2 C_c(\sigma)}{1+\omega^2 R_c^2 C_c^2}. \quad (2)$$

When the frequency is low, $\omega \rightarrow 0$, $Z_2 = R_b + 2R_c$, and when it is very high, $\omega \rightarrow \infty$, $Z_2 = R_b$ (Figure 3).

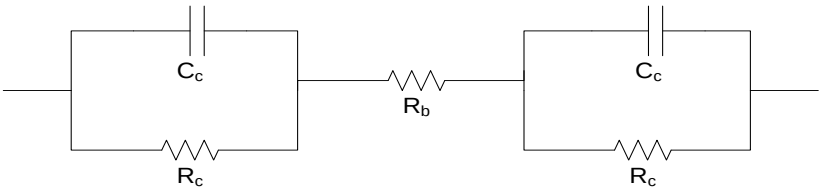

Figure 2 Representative Electrical Circuit for CASE-2

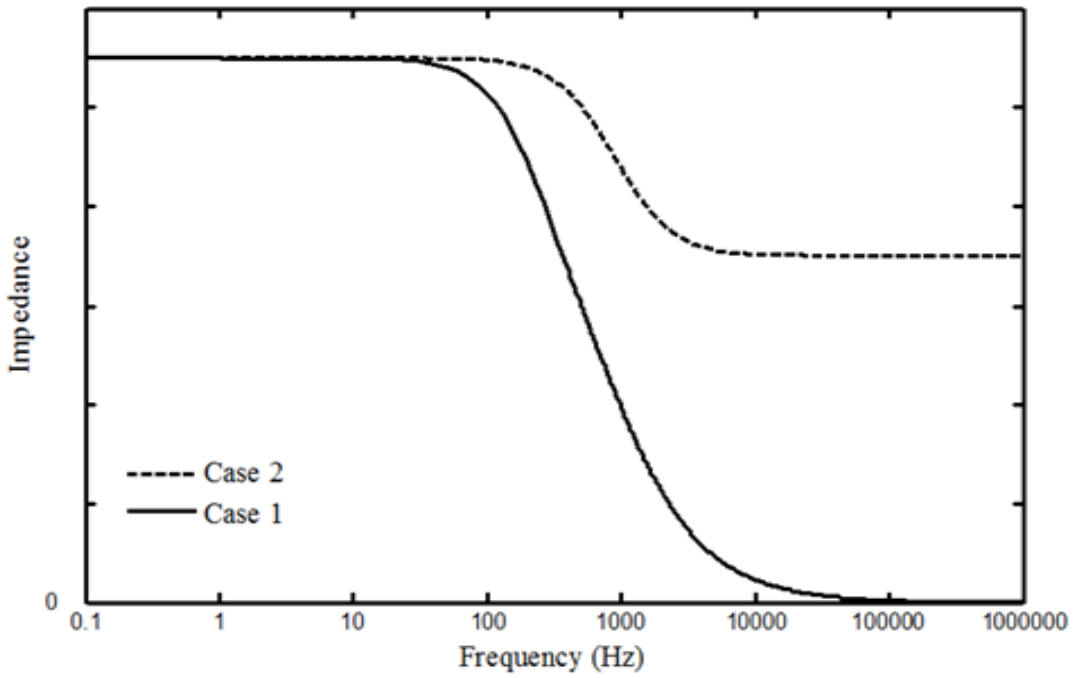

Figure 3 Typical Impedance-Frequency Responses for CASE-1 and CASE-2.

Objectives

The focus was to investigate the effects of adding foam to the smart cement slurry. The specific objectives are as follows:

(i) Characterize and quantify the properties of preformed foam used for preparation of smart foam cement (SFC).

(ii) Characterize the rheological, fluid loss and piezoresistive behavior of SFC slurry with foam contents up to 20% (weight) for cement slurry.

(iii) Model the rheological behavior, fluid loss and piezoresistive behavior of the SFC slurry.

Materials and Methods

Materials

Cement

In this investigation class H oil well cement was used.

Foam

Commercially available foam was used. Based on the manufacturer's data sheet, the major constituents of the foam included water, stearic acid, triethanolamine, sodium sulfate and propane.

Smart Cement (SC)

Class H oil well cement was modified with carbon fibers to make material to be piezoresistive (U.S. Patent 2019). The cement was modified by adding about 0.04% of carbon fibers (CF), by weight of the cement, and the water to cement ratio was 0.38. The SC technology can monitor the changes in the cement at very high magnification of about 2500 times compared to the failure strain after one day curing (Vipulanandan et al. 2015). The main property of interest is piezoresistivity, the change in the resistivity of the cement with the application of the stress. Also, the rheological properties were not affected by the addition of CF (U.S. Patent 2019).

Smart Foam Cement (SFC)

API standard was used to prepare the samples (API 1997). The foam was added to the cement slurry and mixed for at least for 5 minutes. The foam percentage was varied from 0 to 20% by weight of the sample (cement and water).

Methods of Testing

Thermal Property Test

The thermal conductivity was measured using a commercially available device (KD2 Pro thermal property meter). An SH-1 sensor (a 30 mm dual needle) was used after the setting of the SC and SFC. The range of thermal conductivities measured by the analyzer was from 0.02 to 2 W/mK. The operating environment for the device was 0 to 50°C.

Resistivity of Cement Slurry

The digital resistivity meter measured the resistivity directly and the other device, conductivity meter measured the conductivity of the cement slurry and later resistivity was calculated.

Digital meter

This was used to measure the resistivity of the slurries and semi-solids directly. Digital meter measures resistivity up to 400 Ω·m. Suction bulb was used to fill the slurry into the Lucite cell. Slurry was filled and discharged several times before the final fill to avoid air bubble in the sample. Then the sample cell was reattached onto the conductive pins on the meter and reading was taken.

Conductivity Meter

The measurable range was from 0.1 µS/cm to 1000 mS/cm, equivalent to resistivity of 10,000 Ω·m to 0.1 Ω·m. It was first calibrated using standard solution with a known value of conductivity. After calibration, the device was double checked with another standard solution for consistency.

Piezoresistivity Test

When a stress or strain is applied, if the resistivity of the material changes, it represents a piezoresistive material. The piezoresistivity of SC (stress – resistivity relationship) with different foam contents were investigated under compressive loading using the high pressure high temperature (HPHT) apparatus specially designed with probes to measure the changes in electrical resistance. LCR meter (L-inductance; C-Capacitance; R-Resistance) was used with two probes at a frequency of 300 kHz to measure the changes in resistance (Vipulanandan et al. 2013 – 2021).

Rheological test

Using a rheometer in the speed range of 0.3 to 600 rpm (shear strain rate of 0.5 s^{-1} to 1024 s^{-1}) the SFC slurry was characterized. The rheometer was calibrated using standard solutions. Cement slurries were tested 10 minutes after mixing.

Models

Vipulanandan Piezoresistive Slurry Model

The piezoresisitive slurry behavior under uniaxial compressive pressure under laterally confined condition (HPHT device) was modeled using the Vipulanandan Piezoresistive Slurry Model and the relationship is as follows:

$$p = \frac{\frac{\Delta\rho}{\rho_o}}{A - B\frac{\Delta\rho}{\rho_o}} \tag{3}$$

Where $(\Delta\rho/\rho_o)$ is the change in bulk resistivity (decrease), p is the applied pressure in MPa. The model parameters are A and B influenced by the material properties (resistivity, density and others) and testing conditions (temperature and others).

Rheological Model

All the SC and SFC slurries tested showed non-linear shear thinning behavior with a yield stress. Based on the test results, following conditions have to be satisfied for the model to represent the observed behavior and the conditions are as follows:

$$Shear\ stress\ (\tau) = Yield\ stress\ (\tau_0),\qquad When\ Shear\ strain\ rate\ (\dot{\gamma}) = 0$$

$$\frac{d\tau}{d\dot{\gamma}} > 0, \tag{4}$$

$$\frac{d^2\tau}{d\dot{\gamma}^2} < 0, \text{ and} \tag{5}$$

$$\dot{\gamma} \to \infty \Rightarrow \tau = \tau^*. \tag{6}$$

The rheological models used for predicating the shear thinning behavior of SFC slurry are as follows:

Vipulanandan Rheological Model (2014)

The model relationship is as follows (Vipulanandan et al. 2014):

$$\tau - \tau_{o2} = \frac{\dot{\gamma}}{C + D*\dot{\gamma}}, \quad (7)$$

where τ: shear stress (Pa); τ_{o2}: yield stress (Pa); C (Pa. s)$^{-1}$ and D (Pa)$^{-1}$: are model parameters and $\dot{\gamma}$: shear strain rate (s^{-1}).

By applying the conditions from Eqns. (4), (5) and (6) are as follows:

$$\frac{d\tau}{d\dot{\gamma}} = \frac{(C + D\dot{\gamma}) - \dot{\gamma} * D}{(C + D\dot{\gamma})^2} = \frac{C}{(C + D\dot{\gamma})^2} > 0 \Rightarrow C > 0 \quad \text{and}$$

$$\frac{d^2\tau}{d\dot{\gamma}^2} = \frac{-2CD}{(C + D\dot{\gamma})^3} < 0 \Rightarrow D > 0.$$

Also when $\dot{\gamma} \to \infty \Rightarrow \tau_{\max} = \frac{1}{D} + \tau_{o2}$. (8)

Hence there is a limit to the maximum shear stress produced by the SFC slurry.

Artificial Neural Network Modeling

An ANN computational model was used to predict resistivity, piezoresistivity and rheology. Total data sets were used to train the network and for testing the ANN predictions. To design and optimize the solution of ANN, transfer functions must be selected first. Two ANN models were designed for initial investigation. The architecture is set in such a way to select transfer function that gives minimum root mean square error (Figure 4). The following transfer functions were used for ANN prediction.

(i) Sigmoid function given by $f(x) = 1/(1 + e^{-x})$

(ii) Hyperbolic tangent function given by $\tanh(x) = (e^{-2x} - 1)/(e^{-2x} + 1)$

The ANN model was tested for predicting rheology and piezoresistivity data using total of 50 data points. The RMSE (root mean square error) was calculated for ANN model by increasing the number of hidden layers to 4. The ANN model with two layers had the lowest RMSE of 7.17 Pa for the rheology data and 0.30% for piezoresistivity data as shown in Figure 5 and Figure 6 respectively. The coefficients of determination (R^2) were in the range of 0.98 to 0.99 for both rheology and piezoresistivity predictions.

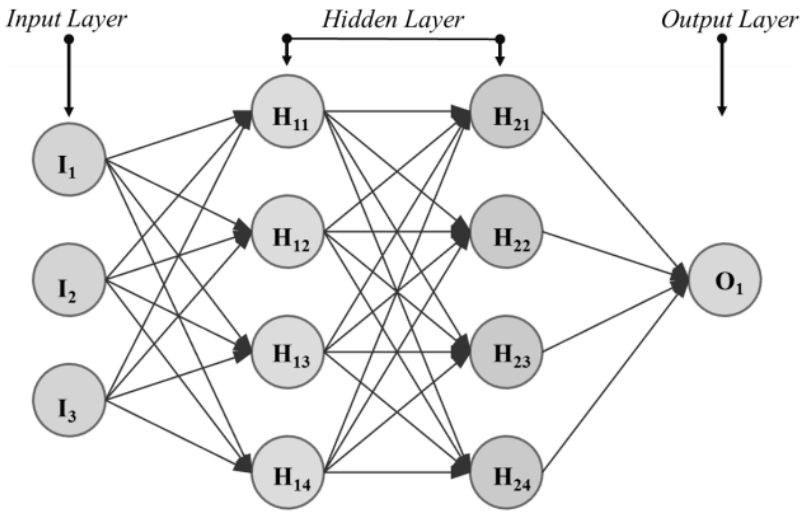

Figure 4 Artificial Neural Network Architecture

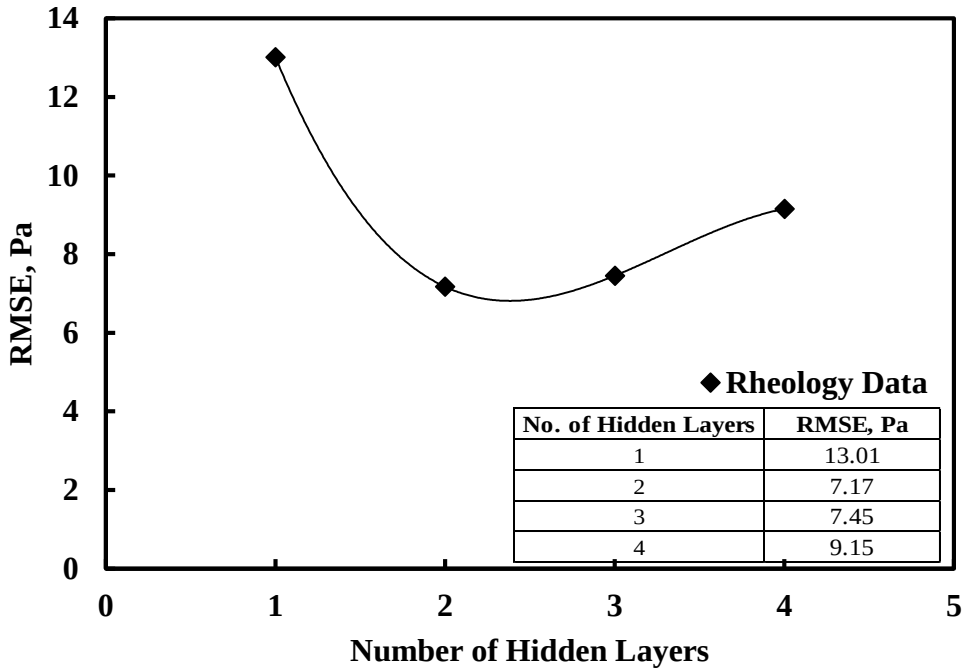

Figure 4 RMSE for the rheological data based on the ANN model predictions with varying amounts of hidden layers.

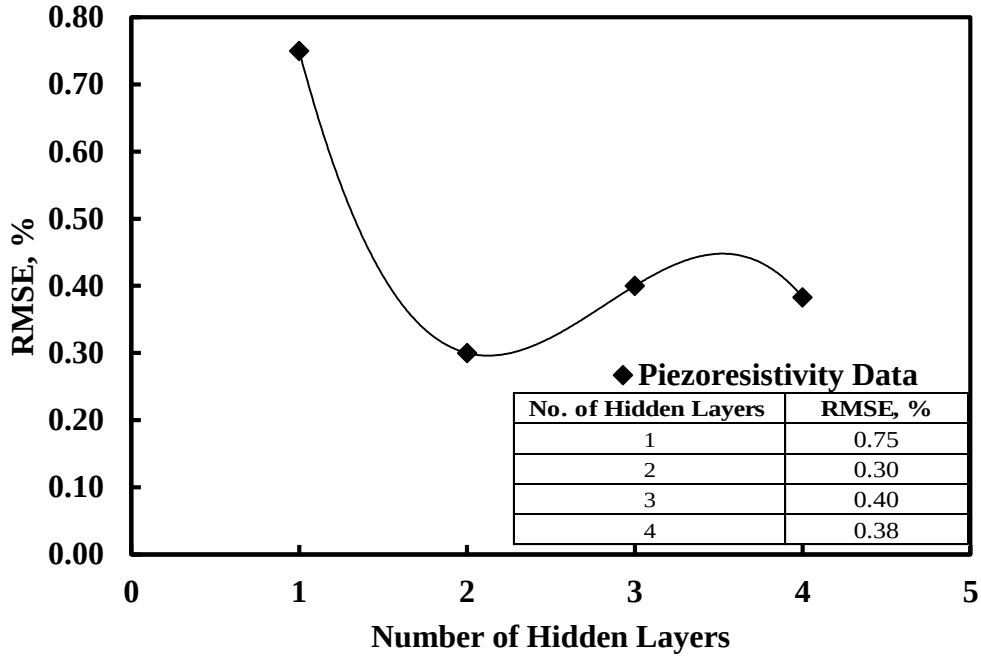

Figure 6 RMSE for the piezoresistivity data based on the ANN model predictions with varying amounts of hidden layers.

Results and Discussion

Characterization of Foam

The stability of the foam is defined by the half-life of the foam which is the time for the foam to collapse to half its height. The stability of the foam was tested using a 50 mL titration tube. The foam experienced a drop in height of 0.3 mL after six hours. The half-life of the foam was greater than 24 hours showing it to be a stable foams. The oxidation reduction potential (ORP) measurement represents the oxidized condition (>0 mV) and reduced condition (<0 mV) in the foam solution. The value of ORP for the foam was -55 mV showed that the foam was in a reduced condition. The pH of the foam was in the range of 8.2 to 8.5 indicating a basic condition. The foam had a unit weight in range of 1.07 to 1.1 kN/m^3. The conductivity of the foam measured using the conductivity probe was in the range of 75 to 120 µS/cm. The resistivity was calculated to be in range of 80 to 135 Ω·m. This shows the presence of air voids since the resistivity of air is in the range of 1.5×10^{13} to 6.0×10^{13} Ω·m (Seran et al. 2013).

Characterizing Smart Foam Cement

Impedance Vs Frequency Curves

The impedance versus frequency relationship was verified immediately after mixing with 20% foam and the response is shown in Figure 7, where the impedance reduced with the increase in the alternative current (AC) frequency and reached a limiting value. The impedance response represents the CASE-2 in **Error! Reference source not found.**,

indicating that the bulk material can be represented by resistance and the material property resistivity. The impedance model better predicted the performance of smart foam cement compared to ANN model.

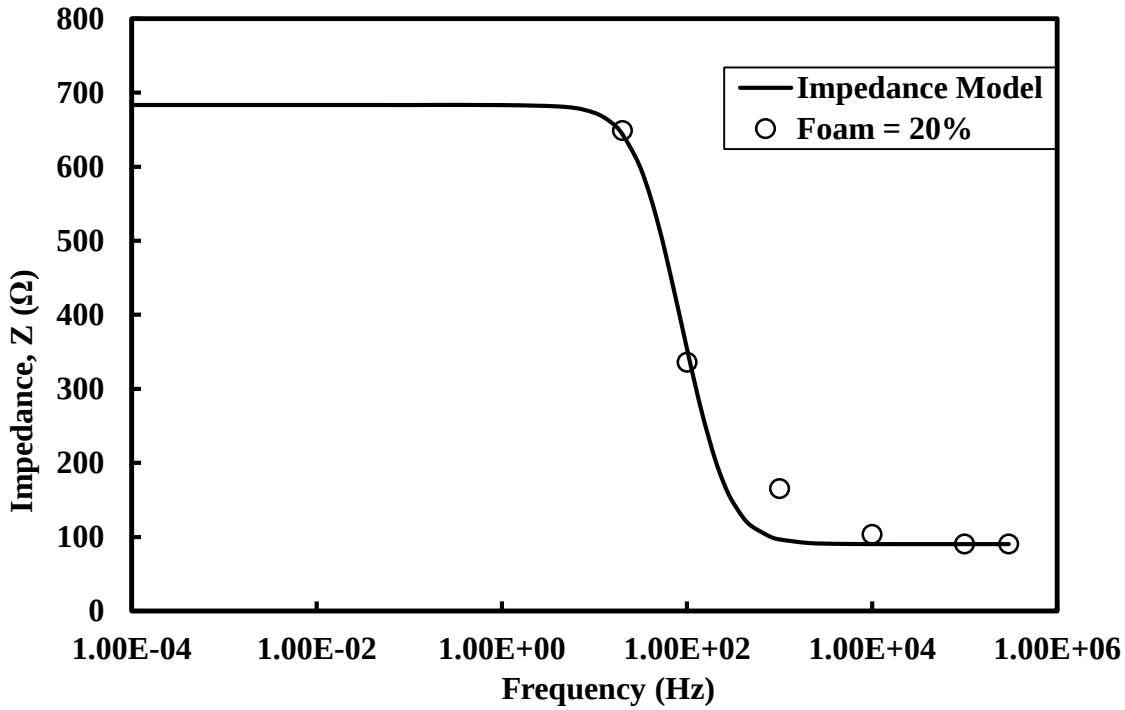

Figure 7 Impedance - Frequency Relationship for the Smart Foam Cement after Mixing

Density

The density of the SC slurry was 1.95 g/cc, and with 5% foam it reduced to 1.53 g/cc, 21.5% reduction. With the addition of 20% foam it reduced the density to 1.07 g/cc, a 45% reduction as shown in Figure 8.

Electrical Resistivity and Quality Control

The initial resistivity of the smart cement immediately after mixing was 1.05 Ω·m as shown in Figure 9 and summarized in Table 1. With the addition of 5% foam, the initial resistivity increased to 1.20 Ω·m, a 14.2% increase. With 20% foam, the initial resistivity increased to 2.04 Ω·m, a 94.3% increase as shown in Figure 8. Hence electrical resistivity will be good quality control parameter in the field.

The variation of electrical resistivity (ρ) with density was found to be nonlinear as shown in Figure 9. Hence it is represented using Vipulanandan correlation model as follows:

$$\rho = \rho_O - \frac{\gamma}{G + H\gamma} \quad (10)$$

where γ is the slurry density in g/cc. The electrical resistivity density model constant ρ_o is 73.93 Ω·m. The model parameters G and H were 0.00045 g/Ω·m.cm^3 and 0.0135 (Ω·m.)$^{-1}$ respectively. The RMSE for the electrical resistivity density model was 0.083 Ω·m.

Table 1 Initial resistivity for smart cement with various foam contents.

Foam Content (%)	Initial Resistivity, ρ_o (Ω-m)
Foam = 0%	1.05 ± 0.03
Foam = 5%	1.2 ± 0.02
Foam = 20%	2.04 ± 0.04

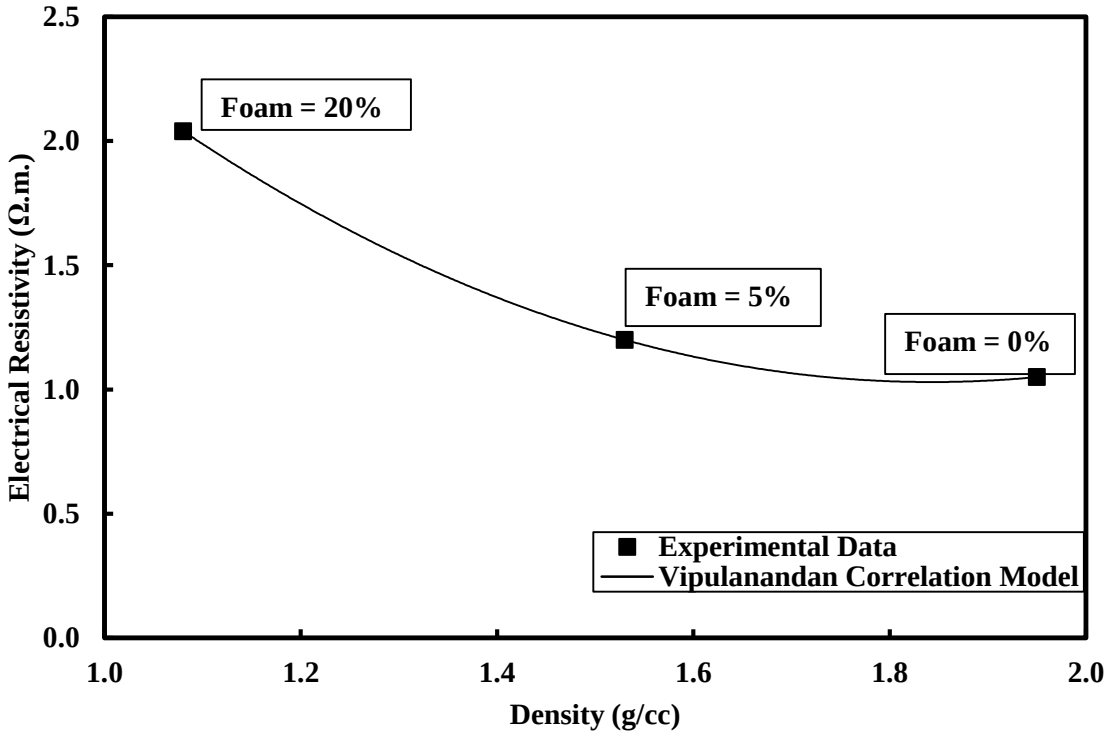

Figure 8 Variation of Initial Electrical Resistivity with Density for the Smart Foam Cement.

Thermal Property

The thermal conductivity of the SC slurry was 0.802 W/mK. With 5% foam (based on total weight of the cement slurry) reduced the thermal conductivity to 0.482 W/mK, 40% reduction. With 20% foam addition it reduced the thermal conductivity to 0.284 W/mK, a 65% reduction as shown in Figure 9.

The variation of thermal conductivity with density was found to be nonlinear (Figure 9). Hence it is represented using Vipulanandan correlation model as follows:

$$K = \frac{\gamma}{I - J\gamma} \qquad (11)$$

where K is the thermal conductivity in W/mK,
γ is the slurry density in g/cc.
The model parameters I and J were 5.68 gmK/Wcm^3 and 1.66 mK/W respectively. The RMSE for the thermal conductivity density model was 0.003 W/mK.

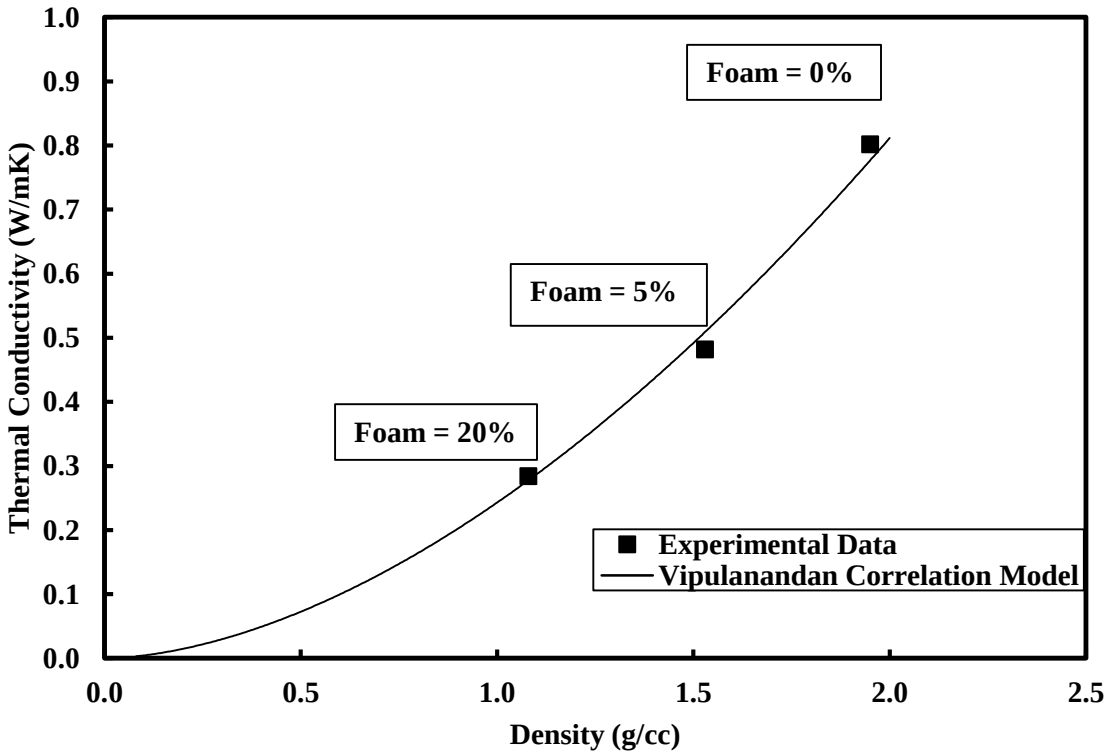

Figure 9 Variation of Initial Themal Conductivity with Density for the Smart Foam Cement.

Piezoresistivity

The SC and SFC slurries were subjected to pressure up to 4 MPa in the high pressure high temperature chamber (HPHT) to investigate the piezoresistive behavior. The model parameters are summarized in Table 2.

0% Foam: The resistivity of the SC slurry decreased nonlinearly with increase in the pressure as shown in Figure 11. The decrease in the resistivity was 8% at 4 MPa pressure, indicating the piezoresistivity characteristics of the smart cement slurry. The value of model parameters A, B are 0.064 % $(MPa)^{-1}$ and 0.0063 $(MPa)^{-1}$. The RMSE for piezoresistivity model was 0.158 MPa while it was 0.077 MPa ANN model. Based on the RMSE, ANN model predicted the test results better than the piezoresistivity model.

5% Foam: The resistivity of the SFC slurry with 5% foam decreased nonlinearly with increase in the pressure as shown in Figure 11. The decrease in resistivity was 12% at 4 MPa pressure, indicating the piezoresistivity characteristics of the SFC slurry. With 5% foam the piezoresistivity characteristics of the SFC slurry increased by 50%. The value of model parameters A, B were 0.075 % (MPa^{-1}) and 0.0041 $(MPa)^{-1}$. The RMSE for piezoresistivity model was 0.145 MPa while it was 0.055 MPa for ANN model. Based on the RMSE, ANN model predicted the test results better than the piezoresistivity model.

20% Foam: The resistivity of the smart cement slurry with 20% foam decreased nonlinearly with increase in the pressure as shown in Figure 10. The decrease in resistivity was 22% at 4 MPa pressure, indicating the piezoresistivity characteristics of the SFC slurry. With 20% foam the piezoresistivity characteristics of the SFC slurry increased by 175%, making the SFC to be more sensing. The value of model parameters A, B were 0.24 % (MPa^{-1}) and 0.0085 $(MPa)^{-1}$. The RMSE for piezoresistivity model was 0.145 MPa while it was 0.145 MPa for ANN model as shown in Figure 10. Based on the RMSE, ANN model predicted the test results as good as the piezoresistivity model.

Table 2 ANN Model and Vipulanandan piezoresistive slurry model parameters.

	ANN Model		Piezoresistivity Model				
Model Parameters	**R^2**	**RMSE**	**A (%.$(MPa)^{-1}$**	**B $(MPa)^{-1}$**	**$(\Delta\rho/\rho)_{max}$ (%)**	**R^2**	**RMSE**
Foam = 0%	**0.99**	**0.077**	**20.26**	**0.0875**	**231.5**	**0.97**	**0.158**
Foam = 5%	**0.99**	**0.055**	**15.13**	**0.051**	**296.7**	**0.99**	**0.145**
Foam = 20%	**0.99**	**0.145**	**8.29**	**0.026**	**318.8**	**0.97**	**0.145**

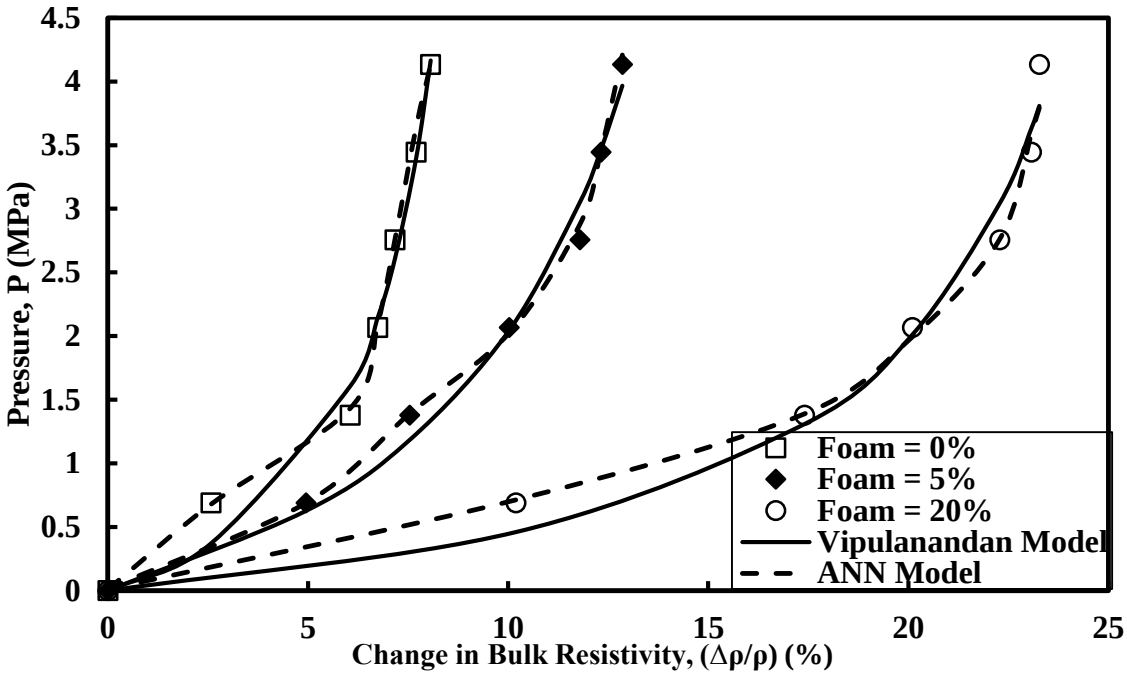

Figure 10 Comparing the Experimental Results to the Model Predictions for the Piezoresistive Responses of the Smart Foam Cement Slurries.

Maximum Change in Resistivity

The piezoresistive model also predicts the maximum percentage change in resistivity with the applied pressure for the SFC and it be equal to the ratio of model parameter A/B when the applied pressure is equal to infinity. The maximum change in piezoresistivity increased with the foam content at summarized in Table 2.

Rheological Properties

Shear stress – shear strain rate relationships for SFC were predicated using the Vipulanandan model and compared with ANN model as shown in Figure 11 In Table 3 all the model parameters are summarized with the RMSE and coefficient of determination for all the SFC slurries.

Vipulanandan Rheological model

0% Foam: The rheological behavior of SC slurry was tested and modeled using the Vipulanandan model (Eqn. (7)) up to a shear strain rate of 1024 s^{-1} (600 rpm). The coefficient of determination (R^2) was 0.98 and the RMSE was 7.43 Pa as summarized in Table 3. The average yield stress (τ_{o1}) for the SC slurry at temperature of 25^{o}C was 28 Pa.

The model parameter C for the cement slurry with w/c ratio of 0.38 at 25°C was 1.97 $Pa.s^{-1}$ as summarized in **Error! Reference source not found.**. The model parameter D for the cement slurry was 0.006 Pa^{-1}. The RMSE was 13.34 Pa and coefficient of determination (R^2) was 0.94 for ANN model (Figure 12). Based on the RMSE, Vipulanandan model predicted the test results better than the ANN model.

5% Foam: The rheological behavior of SFC slurry with 5% foam at a temperature of 25°C was tested and modeled using the Vipulanandan model (Eqn. (12)) up to a shear strain rate of 1024 s^{-1} (600 rpm). The coefficient of determination (R^2) was 0.99 and the RMSE was 3.65 Pa as summarized in Table 3. The average yield stress (τ_{o1}) for the cement slurry at temperature of 25°C was 15 Pa, a reduction of 46% compared to the smart cement without any foam. The model parameter C for the 5% foam cement slurry was 2.34 $Pa.s^{-1}$ an increase of 19% compared to the smart cement without any foam. The model parameter D for the 5% foam cement slurry was 0.009. The RMSE was 3.6 Pa and coefficient of determination (R^2) was 0.98 for ANN model. Based on the RMSE, ANN model predicted the test results better than Vipulanandan model.

20% Foam: The rheological behavior of SFC slurry with 20% foam at a temperature of 25°C was tested and modeled using the Vipulanandan model (Eqn. (12)) up to a shear strain rate of 1024 s^{-1} (600 rpm). The coefficient of determination (R^2) was 0.99 and the RMSE was 2.2 Pa as summarized in **Error! Reference source not found.**. The average yield stress (τ_{o1}) for the cement slurry at temperature of 25°C was 7 Pa, a reduction of 75% compared to the SC without any foam. The model parameter C for the 20% foam cement slurry was 8.49 $Pa.s^{-1}$ an increase of 331% compared to the smart cement without any foam. The model parameter D for the foam cement slurry was 0.01. The RMSE was 2.37 Pa and coefficient of determination (R^2) was 0.98 for ANN model. Based on the RMSE, Vipulanandan model predicted the test results better than the ANN model.

Table 3 ANN Model and Vipulanandan Rheological Model parameters.

	ANN Model		Vipulanandan Model				
Model Parameters	**R^2**	**RMSE**	**C(Pa. s)$^{-1}$**	**D (Pa)$^{-1}$**	**τ (yield)(Pa)**	**τ (max)(Pa)**	**RMSE**
Foam = 0%	**0.94**	**13.34**	**1.97**	**0.0065**	**28.16**	**153.8**	**7.43**
Foam = 5%	**0.98**	**3.6**	**2.34**	**0.009**	**14.73**	**111.1**	**3.65**
Foam = 20%	**0.98**	**2.37**	**8.49**	**0.011**	**7.00**	**90.9**	**2.2**

Maximum shear stress ($\tau_{max.}$)

Based on the Eqn. (8) the Vipulanandan model has a limit on the maximum shear stress ($\tau_{max.}$) the cement slurry at relatively very high rate of shear strains. The τ_{max} for smart cement slurries with 0%, 5% and 20% foam at temperature of 25°C were 153 Pa, 111 Pa and 91 Pa respectively as summarized in Table 3. Hence with 20% foam the maximum shear stress was reduced by 40%.

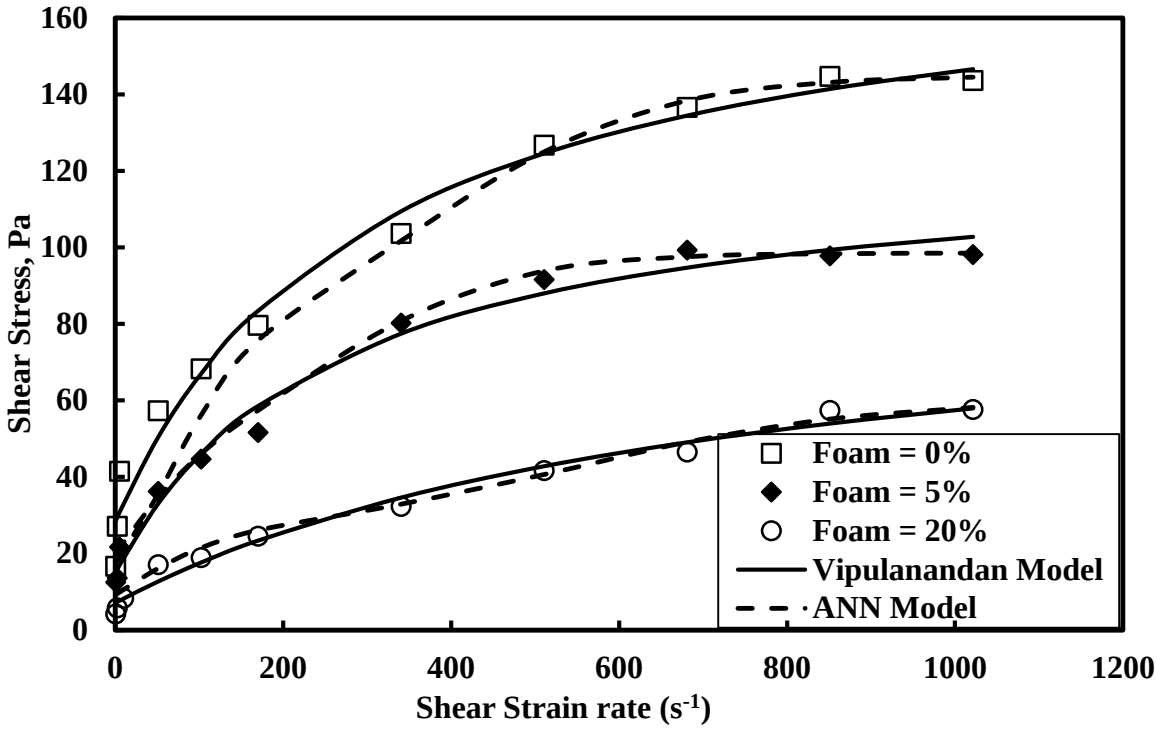

Figure 11 Comparing the Experimental Results to the Model Predictions for the Rheological Responses of the Smart Foam Cement Slurries.

Conclusions

In this study foam was added to the smart cement to develop the light weight smart foam cement. Also, the slurry behavior was modelled using the ANN model and compared to Vipulanandan models. Based on this study, the following conclusions are advanced:

1. The most appropriate equivalent circuit for characterizing smart foam cement based on the impedance frequency response was identified as CASE-2. Hence the smart foam cement can be characterized using the electrical resistivity. Also it has been experimentally proven that resistivity can used for quality control of the smart form cement in the field.

2. With the addition of 20% foam, the density of SFC reduced to 1.07 g/cc, a 45% reduction. The thermal conductivity reduced to 0.284 W/mK, a 65% reduction. The electrical resistivity increased to 2.04 Ω·m, a 94 % increase. Hence the electrical resistivity was a highly sensing parameter.

3. The initial resistivity was correlated to the initial density using the Vipulanandan Correlation Model. Hence by monitoring the resistivity of the smart foam cement density could be predicted. Also the thermal conductivity was correlated to the density.

4. Smart foam cement slurry was piezoresistive and the resistivity change increased with the foam content. With the addition of 20% foam, the resistivity change at 4 MPa (600 psi) increased from 8% for the smart cement slurry with no foam to 22% with 20% foam, about 175% increase in the piezoresistivity. The RMSE for ANN model was between 0.054 to 0.34 and for Vipulanandan piezoresistivity model it was between 0.20 to 1.16. Based on the RMSE values, ANN model predicted better test results than piezoresistivity model.

5. The shear thinning behavior of the smart foam cement slurries have been quantified using the new Vipulanandan rheological model, compared with ANN Model. The RMSE for ANN model was between 2.3 to 13.3 Pa and for Vipulanandan rheological model it was between 2.2 to 7.43 Pa. Vipulanandan rheological model predicted test results better compared to the ANN model.

Acknowledgement

The smart cement study was initiated by the U.S. Department of Energy (DOE) and also the National Science Foundation (NSF) to commercialize the products and technology. The smart foam cement study was also support by the Center for Innovative Grouting and Technology (CIGMAT) and the Texas Hurricane Center for Innovative Technology.

References

[1] Ahmadi, A., Sakib, T., Ghaderi, A. and Beirami, A. (2013). "The Performance of Foam Cement in Iran Oil Wells and Comparison of the Bentonite Light Cement with Foam Cement", Australian Journal of Basic and Applied Sciences, No. 7(4), pp. 696-702.

[2] API Recommended Practice 10B (1997), Recommended Practice for Testing Well Cements Exploration and Production Department, 22nd Edition, American Petroleum Institute, Washington D.C.

[3] Arnavat, M. P., Bruno, J. C. (2015). "Artificial Neural Networks for Thermochemical Conversion of Biomass", Recent Advances in Thermo-Chemical Conversion of Biomass 2015, Pages 133-156.

[4] Bour, D., Rickard, B. (2000). "Application of Foamed Cement on Hawaiian Geothermal Well", Geothermal Resources Council Transactions, Vol. 24, September 24-27.

[5] Carter, K. M. and Oort, E. (2014), Improved Regulatory Oversight Using Real-Time Data Monitoring Technologies in the Wake of Mocondo, SPE 170323, pp. 1-51.

[6] Dahnoune, F., Remini, H., et al (2015). "Ultrasound assisted extraction of phenolic compounds from P. lentiscus L. leaves: Comparative study of artificial neural

network (ANN) versus degree of experiment for prediction ability of phenolic compounds recovery", Industrial Crops and Products 77, pp. 251–261.

[7] Demircan, E., Harendra, S. and Vipulanandan, C.(2011) "Artificial Neural Network and Nonlinear Models for Gelling Time and Maximum Curing Temperature Rise in Polymer Grouts," Journal of Materials in Civil Engineering, Vol. 23, No. 4 , pp. 1-6, 2011.

[8] Dusterhoft, D.M. (2003). "A Comparison between Foamed and Light Weight Cement", Petroleum Society's Canadian International Petroleum Conference, No. 125.

[9] Fuller, G., Souza, P., Ferreira, L. and Rouat, D. (2002). "High-Strength Lightweight Blend Improves Deepwater Cementing", Oil & Gas Journal, Vol. 100, No.8, pp. 86-95.

[10] Glosser, D., Kutchko, B., Benge, G., Crandall, D., Ley, M. T. (2016). "Relationship between operational variables, fundamental physics and foamed cement properties in lab and field generated foamed cement slurries", Journal of Petroleum Science and Engineering, Vol.145, pp. 66-76.

[11] Hammoudi, A., Moussaceb, K. and Dahmoune, F. (2019). "Comparison of artificial neural network (ANN) and response surface methodology (RSM) prediction in compressive strength of recycled concrete aggregates", Construction and Building Materials, Vol. 209, pp. 425–436.

[12] Harms, W.M, Febus, J.S. (1985). "Cementing of Fragile Formations Wells with Foamed Cement Slurries", Society of Petroleum Engineers, SPE-12755-PA, Vol. 37, No. 6, pp. 1049 – 1057.

[13] Harness, P.E. and Sabins, F.L. (1992). "New Technique Provides Better Low Density Cement Evaluation", Society of Petroleum Engineers, SPE-24050-MS, pp. 249 – 258.

[14] Hill, A.D.(1990). "Cement-Quality Logging. Production Logging—Theoretical and Interpretative Elements", Society of Petroleum Engineers, Vol. 14, pp. 123-140.

[15] Ichim, A., Saleh, F. K., Teodoriu, C., Sondergeld, C. (2019) "Investigation of mechanical behavior and physical characteristic of portland cement: Implications for destructive and non-destructive methods", Journal of Petroleum Science and Engineering, Vol.177, pp. 123-134.

[16] Izon, D., Danenberger, E. P. and Mayes, M. (2007). Absence of fatalities in blowouts encouraging in MMS study of OCS incidents 1992-2006. Drilling contractor, 63(4), 84-89.

[17] Labibzadeh, M., Zhhabizadeh, B. and Khajehdezfuly, A., (2010) "Early Age Compressive Strength Assessment of Oil Well Class G Cement Due to Borehole Pressure and Temperature Changes", Journal of American Science, Vol. 6, No.7, pp.38-47.

[18] Loeffler, N.R. (1984). "Foamed Cement; a Second Generation", Society of Petroleum Engineers Conference, SPE-12592-MS, pp. 153-158.

[19] Marriot, T. (2005). "Foamed Conventional Light Weight Cement Slurry For Ultra-Low Density Solves Lost Circulation Problem", SPE Annual Conference, SPE-96108-MS.

[20] McCarter, W. J., Starrs, G., and Chrisp, T. M. (2000). "Electrical conductivity, diffusion, and permeability of Portland cement-based mortars", Journal of Cement and Concrete Research, Vol. 30, pp. 1395–1400.
[21] Mishra, M. and Srivastava, M. (2014). "A View of Artificial Neural Network", IEEE International Conference on Advances in Engineering & Technology Research (ICAETR - 2014), Dr. Virendra Swarup Group of Institutions, Unnao, India.
[22] Ravi, K., McMechan, D. E., Reddy, B. R. and Crook, R. (2007). "Comparative Study of mechanical Properties of Density-reduced Cement Compositions", SPE Drilling & Completion, Vol. 22, No. 2, pp. 119-126.
[23] Rickard, W.M. (1985). "Foam Cement for Geothermal Wells", Transactions, Vol. 9, Part 1, pp. 147-152.
[24] Seran, E., Godefroy, M., Renno, N. and Elliott, H. (2013). "Variations of electric field and electric resistivity of air caused by dust motion", Journal of Geophysical Research: Space Physics, Vol. 118, pp 5358-5368.
[25] Smith, T. and Dolerey, J. (1984). "Foamed Cement Application in Canada", Journal of Canadian Petroleum Technology, Vol. 02, pp. 65 – 70.
[26] Spoerker, H.F. and Doschek, M. (2002). "Field Experience with Applying Foamed Cement Slurries in Mature Depleted Formations", SPE Conference, SPE-77215-MS.
[27] Sugama, T., Brothers, L.E. and Van de putte, T.R. (2005). "Air Foamed Calcium Aluminate Phosphate Cement for Geothermal Wells", Cement and Concrete Composites, Vol. 27, No. 7–8, pp. 758-768.
[28] Thaemlitz, J. and Patel, A.D. (1999). "New environmentally safe high-temperature water-based drilling-fluid system", SPE Drilling & Completion Vol. 14(3), pp. 185-189.
[29] Topcu, I. B., Sardemir, M. (2008). "Prediction of compressive strength of concrete containing fly ashusing artificial neural networks and fuzzy logic", Computational Materials Science, Vol. 41, pp. 305–311.
[30] U.S. Patent (2019) "Chemo-Thermo-Piezoresistive Highly Sensing Smart Cement with Integrated Real-Time Monitoring System" Inventor: C. Vipulanandan, Number 10,481,143 Awarded on November 19, 2019.
[31] Vipulanandan, C. and Prashanth, P. (2013). "Impedance spectroscopy characterization of a piezoresistive structural polymer composite bulk sensor". Journal of Testing and Evaluation, Vol. 41, pp. 898-904.
[32] Vipulanandan, C. and Mohammed, A. (2014). "Vipulanandan rheological model with shear stress limit for acrylamide polymer modified bentonite drilling muds". Journal of Petroleum Science and Engineering, Vol. 122, pp. 38‑47.
[33] Vipulanandan, C, Ramanathan, P. Ali, M., Basirat, B. and Pappas, J. (2015) "Real Time Monitoring of Oil Based Mud, Spacer Fluid and Piezoresistive Smart Cement to Verify the Oil Well Drilling and Cementing Operation Using Model Tests", Offshore Technology Conference (OTC) 2015, OTC-25851-MS.
[34] Vipulanandan, C. and Mohammed, A. (2015). "Smart cement rheological and piezoresistive behavior for oil well applications," Journal of Petroleum Science and Engineering, Vol. 135, pp. 50-58.

[35] Vipulanandan, C. and Mohammed, A. (2015) "Smart cement modified with Iron oxide nanoparticles to enhance the piezoresistive behavior and compressive strength for oil well applications," Journal of Smart Materials and Structures, Vol. 24 (12), 2015, 1-11.

[36] Vipulanandan, C., Ali, K., Basirat, B., Reddy, A. Amani, N., Mohammed, A. Dighe, S., Farzam, H. and W. J. Head (2016), "Field Test for Real Time Monitoring of Piezoresistive Smart Cement to Verify the Cementing Operations ," OTC-27060-MS.

[37] Vipulanandan, C., and Ali, K., (2018a) "Smart Cement Grouts for Repairing Damaged Piezoresistive Cement and the Performances Predicted Using Vipulanandan Models" Journal of Civil Engineering Materials, American Society of Civil Engineers (ASCE), Vol. 30, No. 10, Article number 04018253.

[38] Vipulanandan, C., and Amani, N., (2018b) "Characterizing the Pulse Velocity and Electrical resistivity Changes In Concrete with Piezoresistive Smart Cement Binder Using Vipulanandan Models" Construction and Building Materials, Vol. 175, pp. 519-530**.**

[39] Vipulanandan, C. and Mohammed, A. (2020). "Magnetic Field Strength and Temperature Effects on the Behavior of Oil Well Cement Slurry Modified with Iron Oxide Nanoparticles and Quantified with Vipulanandan Models," Journal of Testing and Evaluation, 48(6), pp.4516-4537.

[40] Vipulanandan, C. and Mohammed, A. (2020) "Effect of drilling mud bentonite contents on the fluid loss and filter cake formation on a field clay soil formation compared to the API fluid loss method and characterized using Vipulanandan models" , Journal of Petroleum Science and Engineering. Vol. 189, Article Number 107029, pp. 1-19.

[41] Vipulanandan, C. (2021) Smart Cement: Development, Testing, Modeling and Real-Time Monitoring, CRC Press, Taylor and Francis Group, 440 pp.

[42] Zhang, J., Qin, L. and Li, Z. (2009). Hydration monitoring of cement-based materials with resistivity and ultrasonic methods. Materials and Structures, 42(1), 15-24.